PHYSICAL REVIEW E **75**, 060901(R) (2007)

Quantification of spatial intensity correlations and photodetector intensity fluctuations of coherent light reflected from turbid particle suspensions

Vinayakrishnan Rajan,* Babu Varghese, Ton G van Leeuwen, and Wiendelt Steenbergen
Biomedical Technology Institute, Biophysical Engineering Group, University of Twente, P.O. Box 217, NL-7500AE Enschede, The Netherlands

(Received 21 July 2006; published 20 June 2007)

We present a model for predicting the spatial intensity correlation function of dynamic speckle patterns formed by light backscattered from turbid suspensions, and an experimental validation of these predictions. The spatial correlation varies remarkably with multiple scattering. The provided computational scheme is a step towards correctly interpreting signals obtained from instruments based on the measurement of dynamic speckle patterns in the far field.

DOI: 10.1103/PhysRevE.75.060901 PACS number(s): 87.64.Cc, 42.25.Kb, 42.30.Ms, 87.15.Aa

In biomedical imaging a number of measurement techniques are based on the spatial and temporal analysis of coherent intensity fluctuations [1–5], also known as dynamic speckle patterns. Dynamic speckle patterns are produced by the interference of coherent waves which are emitted by media with internal motion of scattering particles. Such a speckle pattern depends on several parameters such as the distance from the medium to the detector, the illumination pattern, the absorption level, and the particle size, shape, and concentration. So a system which performs detection of backscattered photons in the far field is also influenced by these parameters. The quantification of such variations is thereby necessary for all the instruments based on imaging dynamic coherent intensity fluctuations on a detector. The laser Doppler perfusion imager (LDPI) is such an instrument, which is based on collecting backscattered photons to construct blood flow maps of an area of tissue. In this instrument, a collimated laser beam illuminates an area of tissue and a detector is used to collect backscattered photons propagated through free air. It is known that the signal from such a system is influenced by the number of coherence areas, or speckles, on the detector [4,6]. The diffusion of temporal field correlations through turbid media, which is also of interest in such imaging systems detecting backscattered photons, was reported earlier [5,7].

The spatial field and intensity correlation of speckles were extensively studied in terms of particle size and concentration [8], distance to the detector [9], scattering angle [10], and angle of rotation of source and sample [11]. Several studies were also reported on the contribution of different correlation ranges [12] and spatial correlation of microwaves [13,14]. In this Rapid Communication we focus on the prediction of the effect of multiple scattering and absorption on the spatial intensity correlation in the far field. Li and Genack [15] showed that the intensity distribution on the output surface due to point excitation and the intensity correlation function on a distant speckle pattern are Fourier transform pairs. We use this result as a building block of a general theoretical framework to predict photocurrent fluctuations generated by dynamic speckle patterns from mixed dynamic-static media illuminated by coherent light. Our model is able to deal with fields generated by different fractions of backscattered photons. These fractions can be defined according to the Doppler shift, number of scattering events, and penetration depth of photons. Our method utilizes an effective amount of speckles on the far-field detector calculated by a weighted integration of the calculated intensity correlations functions. The provided computational scheme is a step towards quantification of speckle effects in instruments based on imaging dynamic coherent intensity fluctuations on a detector.

In the following description, various quantities occur which are indicated and localized in Fig. 1. A component of our theoretical approach is a relation established between the photodetector signal and the two-point statistics of the speckle intensity field. First the space-time correlation function $\Gamma_{II}(\Delta r, \tau)$ of the intensity variations is expressed in terms of the space-time correlation function $\Gamma_{EE}(r, \tau)$ of the electric field by the Siegert relation [16]. An expression for

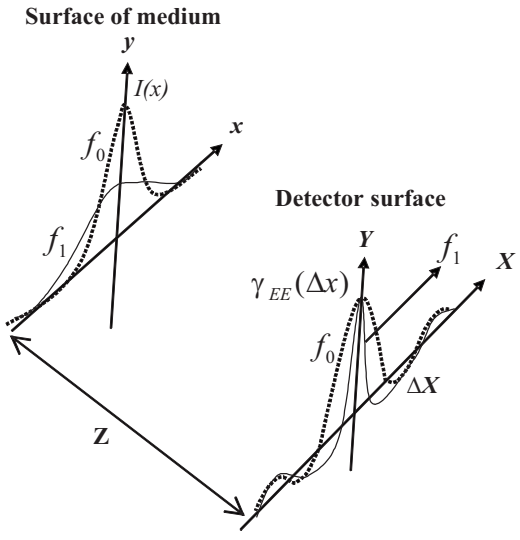

FIG. 1. Illustration of quantities on the surfaces of the medium and the detector; correlation functions for Doppler-shifted and unshifted light fractions f_1 and f_0 on the detector generated by the intensity distributions on the scattering medium surface.

*v.rajan@tnw.utwente.nl

the space-time field correlation coefficient is derived from the correlation functions of Doppler-shifted or non-Doppler shifted fields that together compose the total electric field. Eventually, the variance of photocurrent fluctuations can be written in terms of so-called fractional coherence areas of these composing local field complex amplitudes by [17]

$$\langle i_{\mathrm{ac}}^2 \rangle \equiv \Gamma_{ii}^{\mathrm{ac}}(\tau = 0) = A_{\mathrm{det}} R^2 \langle I \rangle^2 \left[2 \sum_{i}^{M} f_0 f_i A_{\mathrm{coh}}^{0i} + \sum_{i=1}^{M} \sum_{j=1}^{M} f_i f_j A_{\mathrm{coh}}^{ij} \right], \quad (1)$$

where A_{det} is the effective detection area, R is the responsivity of the detector, and $\langle I \rangle$ is the average intensity of the light within the detection area. Furthermore, f_0 is the fraction of non-Doppler shifted photons, while $f_1 \cdots f_M$ represent fractions of Doppler shifted photons that can be defined on the basis of various criteria, such as the Doppler shift, the number of Doppler scattering events, the (optical) path length, and the penetration depth into the medium. A_{coh}^{ij} represents the so-called fractional coherence area on the detector formed by all pairs of photon groups i and j. This can be written in terms of the correlation coefficient of the fields,

$$A_{\mathrm{coh}}^{ij} = 2\pi \int_0^{\infty} \gamma_{EE}^{j}(\Delta x, 0) \gamma_{EE}^{*j}(\Delta x, 0) \Delta x d\Delta x, \quad (2)$$

where Δx is the spatial separation on the detection plane, and γ_{EE}^{j} and γ_{EE}^{j} are the field correlation coefficients of various photon fractions $f_1 \cdots f_M$ of Doppler shifted photons. For $M = 0 \cdots 1$ these are indicated in Fig. 1. It is assumed that the intensity distribution of each photon fraction is homogenous over the detector and is time independent, and that the speckles are isotropic. The latter implies a circular symmetry of the light emitting spot of the turbid medium. Another assumption which has been made in deriving Eqs. (1) and (2) is that the effective photodetection area comprises many coherence areas. This condition is required to allow sufficient spatial averaging of the intensity field to obtain space-time correlations. If this condition is not satisfied, Eq. (1) will adopt a slightly more complicated form, and is only valid if the spatiotemporal intensity fluctuations are ergodic. In most cases the effective photodetector will include sufficient coherence areas or speckles for our theory to be applicable.

Equation (1) can be further simplified if apart from a fraction f_0 of nonshifted photons only a single fraction f_1 of Doppler shifted photons is specified, which gives for Eq. (1) with $M = 1$

$$\langle i_{\mathrm{ac}}^2 \rangle = A_{\mathrm{det}} R^2 \langle I \rangle^2 [2 f_0 f_1 A_{\mathrm{coh}}^{01} + f_1^2 A_{\mathrm{coh}}^{11}]. \quad (3)$$

Equation (3) gives the mean square value of photocurrent fluctuations in terms of correlation functions of one group of unshifted photons and one group of Doppler shifted photons. This will occur in mixed static and dynamic media such as skin which reflect a combination of photons with nonzero and zero Doppler shift depending on the optical properties and blood volume.

In order to predict the coherence area we need to express the spatial correlation functions γ_{EE}^{j} on the detector, as appearing in Eq. (2) in terms of the light backscattered by the medium. Figure 1 illustrates the situation. Here intensity distributions $I(x,y)$ of non-Doppler shifted and Doppler shifted photon fractions f_0 and f_1 are indicated on the surface of the medium, along with their correlation functions $\gamma_{EE}(\Delta X)$ on the detector. Since this can be considered as the problem of far-field spatial coherence on a screen illuminated by a spatially incoherent, quasimonochromatic source, the Zernike-Van Cittert theorem [18] can be applied here, as was shown in Ref. [15]. This implies that the spatial correlation function of the field on the detector can be determined from the Fourier transform of the intensity distribution on the remote diffusely reflecting medium. Hence if the irradiance distribution on the source is $I(x,y)$, the spatial field correlation on the detector can be written as

$$\gamma_{EE}(\Delta X, \Delta Y) = \frac{\int\int_{\mathrm{source}} I(x,y) \exp\left[-i \frac{2\pi}{\lambda Z} (x \Delta X + y \Delta Y) \right] dx dy}{\int\int_{\mathrm{source}} I(x,y) dx dy} \quad (4)$$

with x, y, ΔX, and ΔY the positions on the surface of the turbid medium, and spatial separations on the plane of detection, respectively, Z the distance of the medium to the detector plane, and λ the wavelength of light in the transparent medium between the turbid medium and the detector. So if the irradiance distribution function of two fractions of the outgoing light on the surface of the medium is known, the fractional coherence area on the detector can be calculated by substituting the correlation coefficients obtained from Eq. (4) in Eq. (2).

In our approach, we predict the irradiance distribution from a scattering medium with the Monte Carlo simulation technique which allows us to construct irradiance distributions for specific photon fractions. From the photon model we switch to the wave picture of light by application of the Zernike-Van Cittert theorem as expressed by Eq. (4). This switch is made by depicting each photon that is simulated to transit the interface between the turbid medium and the surrounding medium to emit a spherical wave from the surface of the medium, independent of its k-vector on transition in the Monte Carlo simulation. Hence it is assumed that the k-vectors of all photons leaving the turbid medium are more or less isotropically distributed, so that a photon with a specific k-vector is representative of all photons transiting the interface at that specific position.

In this Rapid Communication we validate our approach for the case of completely dynamic particle suspensions. By assuming all photons to be Doppler shifted (hence $f_0 = 0$ and $f_1 = 1$), and normalizing with $\langle i_{\mathrm{dc}} \rangle = R \langle I \rangle A_{\mathrm{det}}$, Eq. (3) can be written as

$$\frac{\langle i_{\mathrm{ac}}^2 \rangle}{\langle i_{\mathrm{dc}} \rangle^2} = \frac{A_{\mathrm{coh}}}{2 A_{\mathrm{det}}}. \quad (5)$$

Equation (5) is valid for a nonpolarized speckle pattern. Here a factor of 2 is introduced in the denominator, since a non-

polarized speckle pattern is a summation of two independent orthogonally polarized patterns which are formed by multiple scattering. Experimentally the coherence area A_{coh}, or effective speckle size, can be estimated from the modulation depth of the photocurrent intensity fluctuations by using Eq. (5).

For validation we compare the calculated coherence area based on Eqs. (2) and (4) with the experimental one based on Eq. (5), using the ac and dc photodetector signals as input. In our experiment we illuminate the medium with a laser beam at normal incidence and collect the backscattered photons using a lens of focal length 30 mm, placed at a position of 26 cm from the front surface of the scattering medium, that focuses the light on a photoreceiver. The setup and the signal acquisition have been described in more detail in Rajan *et al.* [6]. A cubic glass cuvette of 8 ml is used as a sample holder. Water suspensions of Polystyrene microspheres (Polysciences Inc.) with diameters (⌀) of 0.202 μm (anisotropy factor g=0.3), 0.771 μm (g=0.9), and 1.53 μm (g=0.93) are used to make scattering phantoms. Samples with reduced scattering coefficients (μ_s') of 0.5, 1, 2, 3, and 4 mm^{-1} are made from each particle suspension, based on scattering cross sections following from Mie theory calculations, taking into account the wavelength of the laser light of 632.8 nm and the refractive index of water. Ecoline Black dye (Talens) is added to get absorption coefficient μ_a=0.02 mm^{-1}.

In the Monte Carlo simulation [19] the scattering phantom is defined as a semi-infinite layer. The optical properties are defined as that of the experimental phantoms. Since the scattering properties and the particle number density of calibrated polystyrene sphere suspensions as used in this study are well-known, it is possible to exactly mimic these properties in simulations. A collimated Gaussian beam with different beam diameters is used as the source and is positioned perpendicular to the interface of the medium. In typical diagnostic tissue imaging systems [3,4], the photons are detected at a relatively large distance from the sample. In principle, the correlation coefficient can also be calculated on the basis of the angular intensity distribution of photons arriving at the location of the lens. However, when this detection configuration would be exactly mimicked in the simulation, almost no simulated photons would be detected. For this reason the simulated detector was positioned just above the medium and all the photons that are emitted by the medium are regarded as detected.

Simulations are performed on the above configuration and particle suspensions. Each simulation includes 60 000 detected photons. The resulting backscattered intensity distributions are used to calculate the spatial coherence of the field by applying Eq. (4), using the distance from the medium to the detector in the experimental setup. The A_{det} used is the area of the lens (95 mm^2) in front of the photodetector. It was shown earlier [6] that focusing light to within the physical borders of a photodetector will give the same modulation depth as when the lens is replaced with a photodetector of similar size.

Figure 2 shows the coherence area vs the reduced scattering coefficient for different beam diameters, for the ⌀0.771 μm particle suspension. It is observed that the variation in scattering level results in a considerable variation of

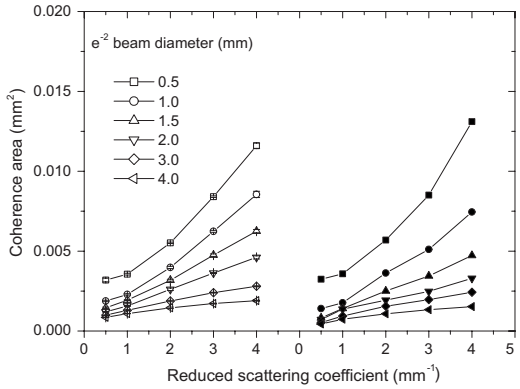

FIG. 2. Coherence area as a function of reduced scattering coefficient and intensity profiles for a particle suspension of ⌀0.771 μm (scattering anisotropy g=0.9). Left: measurement and Right: simulation.

coherence area. Moreover, the variation in coherence area due to variation in scattering level decreases with increasing beam diameter. As the scattering level increases, the number of speckles on the effective detector decreases, since the higher scattering level results in a narrow backscattered intensity distribution. This variation is larger for narrow beams than for wide beams, since the relative change of the width of the intensity distribution by variation in the scattering level is larger for narrow beams than for wide beams. For wide beams the speckle number variation by scattering level variations is suppressed. The same kind of variation is also seen in the plot of the ⌀1.53 μm particle suspension (Fig. 3). Our theoretical calculations match with the experimental results. We correctly predicted the coherence area for a range of scattering anisotropies, scattering levels, and beam sizes. It can be said from the results for the anisotropic particles, with anisotropy factors resembling those of biological tissue, that the spatial correlation varies considerably with scattering level and this variation is very low for broad intensity profiles.

Figure 4 shows the coherence area plot for the ⌀0.202 μm particle suspension. It can be observed that for this more isotropically scattering particle, the spatial correla-

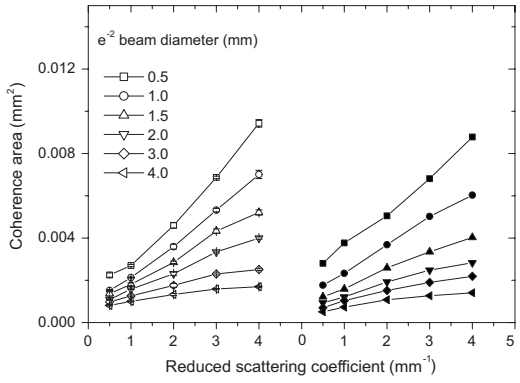

FIG. 3. Coherence area as a function of reduced scattering coefficient and intensity profiles for a particle suspension of ⌀1.53 μm (g=0.93). Left: measurement and Right: simulation.

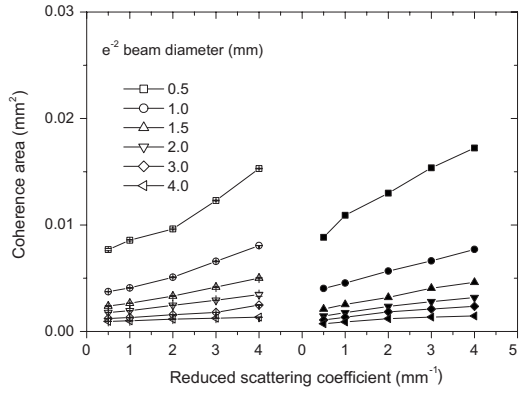

FIG. 4. Coherence area as a function of reduced scattering coefficient and intensity profiles for a particle suspension of ⌀0.202 μm (g=0.32). Left: measurement and Right: simulation.

tion plot for a single beam diameter shows less variation compared to that of anisotropic particles. Furthermore, for this medium the coherence areas are larger than for the media with higher scattering anisotropy. For large particle sizes with g=0.9 and 0.93 the coherence area varies by a factor of 4 for a 0.5 mm beam in the experiment as well as the simulation. For the ⌀0.202 μm particle suspension the coherence area variation for a narrow beam is only a factor of 2. This is because for this medium low order, scattering is dominant and is contributing significantly to the intensity distribution on the surface of the medium, hence the relative change of the width of the backscattered intensity distribution with increasing scattering level is small. Our theoretical calculation agrees well with experimental results even though we are not considering a polarization factor in applying Eq. (5). For smaller particles a better quantification can be done by taking polarization into consideration. For this our model can be further extended by considering the contribution from two fractions of backscattered photons in Eq. (2), one is polarized and the other one is nonpolarized.

In conclusion we have shown that the coherence area detected in reflection mode in the far field of a turbid medium can be predicted with a sequence of models using the photon and wave picture of light. Our theory was able to predict the different behavior for anisotropic as well as isotropic scatterers. It is shown that the spatial correlation varies considerably with diffuse scattering, a variation which can be suppressed by using broader intensity profiles. The theoretical and numerical method will improve the interpretation of results obtained from coherence-based biomedical imaging instruments based on measuring dynamic speckle patterns in the far field. It will, for instance, allow us to quantify the effect of spatial variations in tissue optical properties on the results obtained with such imaging instruments.

This research was sponsored by the Netherlands Technology Foundation STW under Grant No. TTF.5840.

[1] H. Fujii, K. Nohira, Y. Yamamoto, H. Ikawa, and T. Ohura, Appl. Opt. **26**, 5321 (1987).
[2] J. D. Briers and S. Webster, Opt. Commun. **116**, 36 (1995).
[3] T. J. H. Essex and P. O. Byrne, J. Biomed. Eng. **13**, 189 (1991).
[4] K. Wårdell, A. Jakobsson, and G. E. Nilsson, IEEE Trans. Biomed. Eng. **40**, 309 (1993).
[5] D. A. Boas, L. E. Campbell, and A. G. Yodh, Phys. Rev. Lett. **75**, 1855 (1995).
[6] V. Rajan, B. Varghese, T. G. van Leeuwen, and W. Steenbergen, Opt. Lett. **31**, 468 (2006).
[7] G. Maret and P. E. Wolf, Z. Phys. B: Condens. Matter **65**, 409 (1987).
[8] Y. Piederrière, J. Cariou, Y. Guern, B. Le Jeune, G. Le Brun, and J. Lotrian, Opt. Express **13**, 5030 (2005).
[9] A. Apostol and A. Dogariu, Phys. Rev. Lett. **91**, 093901 (2003).
[10] B. Hoover, J. Opt. Soc. Am. A **16**, 1040 (1999).
[11] I. Freund, M. Rosenbluh, and S. Feng, Phys. Rev. Lett. **61**, 2328 (1988).
[12] A. Z. Genack, N. Garcia, and W. Polkosnik, Phys. Rev. Lett. **65**, 2129 (1990).
[13] P. Sebbah, B. Hu, A. Z. Genack, R. Pnini, and B. Shapiro, Phys. Rev. Lett. **88**, 123901 (2002).
[14] A. García-Martín, F. Scheffold, M. Nieto-Vesperinas, and J. J. Sáenzl, Phys. Rev. Lett. **88**, 143901 (2002).
[15] J. H. Li and A. Z. Genack, Phys. Rev. E **49**, 4530 (1994).
[16] B. J. Berne and R. Pecora, *Dynamic Light Scattering: With Applications to Chemistry, Biology and Physics* (Wiley, New York, 1976).
[17] A. Serov, W. Steenbergen, and F. F. M. de Mul, J. Opt. Soc. Am. A **18**, 622 (2001).
[18] M. Born and E. Wolf, *Principles of Optics* (Pergamon, New York, 1975).
[19] F. F. M. de Mul, M. H. Koelink, M. L. Kok, P. J. Harmsma, J. Greve, R. Graaff, and J. G. Aarnoudse, Appl. Opt. **34**, 6595 (1995).